Arabian Journal for Science and Engineering (2022) 47:12555–12568
https://doi.org/10.1007/s13369-021-06554-y

RESEARCH ARTICLE-CIVIL ENGINEERING

# Microstructural Evaluation of the Effect of Initial pH on Geotechnical and Geoenvironmental Characteristics of Marl Soils

**M. Amiri**[1] · **R. Salehian**[1]

Received: 27 September 2021 / Accepted: 27 December 2021 / Published online: 17 January 2022


## Abstract

The present study aims at studying the effect of initial pH on some geotechnical and geoenvironmental properties of marl soils. For this purpose, marl soils with different initial pHs were prepared by adding 1 M sodium alkali hydroxide (NaOH) and hydrochloric acid (HCl). Changes in geotechnical and geoenvironmental characteristics were investigated by macrostructural experiments (Atterberg Limits, permeability and unconfined compressive strength) as well as microstructural experiments (laser diffraction particle size analysis, XRD, XRF, carbonate percentage determination and SEM images), and the effect of initial soil pH change on marl engineering behavior was investigated. One of the most important results of the present study is changes in the morphology and classification of marl soil with changes in the initial pH. Due to the decrease in initial pH, with the removal of carbonate from the marl soil structure at pH 4, the liquid limit and the plastic limit increased by 19 and 8 units, respectively, and the permeability coefficient ($11.7 \times 10^{-9}$ m/s) decreased by 12 times ($0.99 \times 10^{-9}$ m/s). Also, the unconfined compressive strength reached 0.26 MPa with a 70% reduction at the initial pH of 4. The results of XRD and SEM indicated the stability of palygorskite clay minerals in acidic and alkaline environments. Changing in behavior and classification of marl soil at different initial pHs can be very important in designing geotechnical projects.

**Keywords** Marl · pH · Compressive strength · Microstructure · Soil classification · XRD

## Abbreviations

| | |
|---|---|
| °C | Celsius |
| Å | Angstrom |
| $Al_2O_3$ | Aluminum oxide |
| ASTM | American Society for Testing and Materials |
| C | Cohesion |
| Ca | Carbonate |
| CaO | Calcium oxide |
| CH | High-plasticity clay |
| Cl | Chloride |
| CL | Low-plasticity clay |
| CL-ML | Silty clay |
| CpS | Counts per second |
| *D* | Dolomite |
| $D_{10}$ | The effective size |
| $D_{20}$ | 20% of the soil particles are finer than this size |
| $D_{50}$ | Median grain size |
| $D_{70}$ | 70% of the soil particles are finer than this size |
| $D_{90}$ | 90% of the soil particles are finer than this size |
| EC | Electrical conductivity |
| $Fe_2O_3$ | Iron(III) oxide |
| $G_s$ | Particles density |
| h | Hour |
| $K_2O$ | Potassium oxide |
| Kaol | Kaolinite |
| LL | Liquid limit |
| LOI | Loss on ignition |
| MgO | Magnesium oxide |
| MH | Elastic silt |
| $Na_2O$ | Sodium oxide |
| $P_2O_5$ | Phosphorus pentoxide |
| Pal | Palygorskite |
| PI | Plasticity Index |
| PL | Plastic limit |
| Q | Quartz |
| SEM | Scanning electron microscopy |
| Sep | Sepiolite |
| $SiO_2$ | Silicon dioxide |

✉ M. Amiri
amirii@hormozgan.ac.ir

[1] Faculty of Engineering, University of Hormozgan, Bandar Abbas, Iran

| | |
|---|---|
| $SO_3$ | Sulfur trioxide |
| $TiO_2$ | Titanium dioxide |
| UCS | Unconfined compressive strength |
| USCS | Unified Soil Classification System |
| XRD | X-ray diffraction spectroscopy |
| XRF | X-ray fluorescence |
| $\gamma d$ | Dry density |
| $\Phi$ | Friction angle |
| $\omega$ | Optimum water content |

## 1 Introduction

Marls are among the most abundant deposits in nature. Marl soil has been found in many parts of the world, including Iran, Iraq, Italy, Spain, the UK, Germany, Greece and Canada [1–5]. As sedimentary soils or rocks, marls contain 35–65% clay and calcium carbonate. Marl is known as one of the most sensitive geotechnical formations against erosion and weathering [6]. Therefore, the use of this type of soil in geotechnical projects has created many challenges.

The behavioral characteristics of marl typically depend on the distribution and size of the particles and their plastic properties, in such a way that under dry conditions, the deformation of marl soil is due to the breakdown of particles and the creation of a new structure. However, when this type of soil is exposed to moisture, the bond between the aggregates will degrade and cause swelling in the soil and, at the same time, a change in its hardness and strength [7–9]. The clayey part of marl generally consists of palygorskite and sepiolite [10]. Palygorskite is a type of hydrated magnesium, aluminum and silicate with fibrous structure and morphology. This mineral has a high specific surface area and a porous structure [11–14].

The most common carbonate minerals found in marl are calcite ($CaCO_3$) and dolomite [15]. Carbonate minerals have higher solubility compared to silica minerals and are the most important soluble component in the soil solubility phase [16].

Industrial pollution of water and soil is one of the major environmental problems in human societies, which has attracted the attention of many researchers [17–19]. Industrial wastewater and the pollution from acidic and alkaline wastewater enter the water, and this polluted water possibly leaks into the soil. In a short time, soil pore water quality will affect soil properties [20, 21].

Considering the growing trend of soil and water pollution in recent years, much research has been performed on the impact of chemicals on soil properties [22–27]. Soil pH is one of the important indices in the field of pollution, especially when the environmental pH changes. This pH change can also affect the geotechnical and geoenvironmental characteristics [28, 29]. One of the most probable changes due to pH changing is changes in soil classification, which studies have been conducted by [30, 31] in this regard, and based on these studies, the increase in the pH value with increasing sulfate content was pronounced and in the absence of sulfates, and the soil classification of both clayey soils tended to be transformed according to the USCS. The utilization of lime alone or in combination with natural pozzolana transformed the gray soil (classified as clay of high plasticity) and red soil (classified as clay of low plasticity) to silt class of high plasticity.

Many studies have been performed on the effect of initial pH on the mechanical behavior and various properties of soil [32, 33]. Lowering the pH increases the concentration of hydrogen ions and the level of positive charge at the edge of clay platelets, which leads to their adsorption into the surface containing the negative charge of the other platelets. In this case, the clay particles get closer to each other, and the sedimentation rate of the particles increases, and the soil structure becomes aggregated. Meanwhile, the increase in pH and alkaline conditions in the soil causes the particles to disperse [57]. Studies on the effect of pH indicate that the crystal lattice of the clays is affected by the acidity of the pore water so that with increasing $pH \geq 12$, the solubility of quadrilateral silicate and octahedral aluminate platelets increases [34].

Because various industries are producing pollutants on marl substrates, there is a high possibility of leakage of these pollutants into the substrate soil structure and a change in substrate soil pH. Despite extensive studies in recent years on the interaction of soil and pollution, no significant research has been performed to investigate the effect of initial pH on the geotechnical and geoenvironmental parameters of marl soils. Therefore, the purpose of this study is to investigate the effects of initial pH on the geotechnical and geoenvironmental properties of marl soil from a microstructural perspective.

## 2 Materials and Methods

### 2.1 Marl Soil

The soil used in this study is a marl sample in southern Iran, which is located on the northern shore of the Persian Gulf and west of Bandar Abbas. This region was selected due to the presence of various industries and the possibility of change in the pH of marl soil over time. Most of the experiments performed in this study are based on the ASTM standard and the guidelines of McGill University, Canada, for geoenvironmental experiments. According to the Unified Soil Classification System (USCS), marl is a type of clay of low plasticity (CL) with 98% by weight passing through the sieve no. 200 (corresponding to a 74 μm nominal Sieve Opening). Table 1 presents some geotechnical properties of marl.

**Table 1** Some of the geotechnical properties of marl in southern Iran

| Geotechnical properties | Quantity measured | References for method of measurement |
|---|---|---|
| Clay fraction< 5 μm (%) | 87.9 | ASTM, C1070-01 (ASTM C1070-01, 2014) |
| pH (1:10; soil: water) | 8.5 | ASTM D4972 (ASTM, 2016) |
| EC (1:10; soil: water) (mS/cm) | 6.45 | ASTM D1125-95 (ASTM, 2016) |
| Carbonate content (%) | 31 | Hesse, 1971 (Hesse, 1971) |
| Strength parameters | | |
| Cohesion (MPa) | 0.014 | ASTM D3080 (ASTM, 2016) |
| Friction angle (ϕ°) | 16.7 | |
| Unconfined compression strength (MPa) | 0.87 | ASTM D2166-06 (ASTM, 2016) |
| Liquid limit (%) | 46 | ASTM, D4318 (ASTM, 2016) |
| Plastic limit (%) | 25 | ASTM, D4318 (ASTM, 2016) |
| Plasticity index (%) | 21 | ASTM, D4318 (ASTM, 2016) |
| Maximum dry density (kN/m$^3$) | 16.5 | ASTM D698 (ASTM, 2016) |
| Optimum water content (%) | 16 | ASTM D698 (ASTM, 2016) |
| Permeability coefficient (m/s) | $1.2 \times 10^{-08}$ | ASTM D2434 (ASTM, 2016) |
| Particles density $G_s$ | 2.65 | ASTM, D854 (ASTM, 2016) |
| Classification | CL | ASTM, D3282 (ASTM, 2016) |
| Color | Green | |
| Mineral composition using XRD analysis | Palygorskite, sepiolite, kaolinite, calcite, dolomite, quartz | (Ichimura and B Manning) |

In the presented analysis, the calcium oxide content of natural marl is 15.91%. The XRF test was performed with an X-ray fluorescence device model PW1410 made by the Dutch company PHILIPS (Table 2).

## 2.2 Sample Preparation

The marl used in this study has an initial pH of 8.5, which is the natural pH of marl soil. In this paper, sodium hydroxide (NaOH) and hydrochloric acid (HCL) solutions prepared by Merck are used to create acidic and alkaline conditions. In order to prevent the shock caused by the pH change and its effect on the soil structure, low concentrations (1 M) of NaOH and HCL solutions were used to change the pH. The final pH of the sample after adding acidic and alkaline solutions is called the stabilized pH. To stabilize the initial pH of the marl, 3 kg of dry soil passing through sieve no. 40 was set apart, and a water–soil suspension with the ratio of 1:5 (5 distilled water:1 soil) was made. The resulting suspension was stirred for 3 h and then stored for 24 h. Then, to stabilize the marl samples at pH 2, 4, 6, and 11, 1 M sodium hydroxide and hydrochloric acid solutions were added dropwise to the water–soil mixture using a pipette. It took 2 h for the acidic conditions to be reached in the soil. pH changes were not more than 0.2 units per hour. Also, for obtaining alkaline conditions, 1 h was taken for the pH to increase by one unit. Each sample had about 1 unit of pH return the next day. After about 20 days, the pH of the samples was stabilized at the desired pH, and then, the process of leaching and acid and alkali addition was performed on the soil every other day. These steps were repeated daily for about 4 months until the pH of the samples remained constant at the desired level for 72 h.

For drying, the samples were poured into glass containers and placed in an oven at 60 °C. It is worth noting that the pH changes are done in several stages, and for every 2 units of pH change after the pH is stabilized, the samples are leached and dried at 60 °C. According to the fact that in the leaching and adding acid stages, due to the dissolution of carbonate in the presence of acid, carbonate is removed from the soil structure. At the end of the leaching and drying stages, about 1.5 kg of dry soil was obtained for each 3 kg of soil. In each stage of soil sample preparation, in addition to measuring pH changes, samples were also prepared for the X-ray diffraction test. After the samples were dried off, their pH was measured again according to the ASTM D4972 standard. The samples were stirred at a ratio of 1–10 (1 soil: 10 distilled water) for 3 h using an electric stirrer and were stored for 96 h to fully homogenize the system and perform the necessary cation exchange. After this period, the pH was measured

**Table 2** Chemical characteristics of marl (southern Iran) based on XRF analysis

| Materials | Chemical compositions (%) | | | | | | | | | | | |
|---|---|---|---|---|---|---|---|---|---|---|---|---|
| | $SiO_2$ | $Al_2O_3$ | $Fe_2O_3$ | CaO | MgO | $K_2O$ | $Na_2O$ | $TiO_2$ | $SO_3$ | $P_2O_5$ | Cl | Loss on ignition |
| Natural Marl | 33.46 | 9.32 | 4.48 | 15.91 | 6.02 | 1.57 | 3.21 | 0.44 | 0.67 | 0.14 | 1.15 | 23.63 |

**Table 3** Initial and final pHs of marl soil samples after drying

| Initial pH | Final pH |
|---|---|
| 2 | 3.8 |
| 4 | 6.4 |
| 6 | 7.4 |
| 8.5 | 8.5 |
| 11 | 10.1 |

using a Lovibond SensoDirect 150 pH meter. Table 3 shows the initial and final pHs of the soils. It can be seen that after the soil dries, the pH of the suspension changes slightly due to the high percentage of carbonate in the marl sample. So, the pH increases from 2 to 3.8, while the pH of the suspension decreased from 11 to 10.1.

### 2.3 Methodology

To determine the percentage of marl carbonate in soil, a test was performed for determining the percentage of carbonate (titration) by adding hydrochloric acid (HCl) and sodium hydroxide (NaOH) to the samples [35]. Also, to determine the effect of pH on the microstructural properties of marl, X-ray diffraction (XRD), X-ray fluorescence (XRF), scanning electron microscopy (SEM) and particle size analysis (PSA) were performed.

PSA test [36] was used to determine the particle size distribution of the samples. In this experiment, the particle size distribution was determined using a neon–helium laser beam and a wet system. In this method, the samples were suspended (alcohol) in glass containers. The mixture was then placed on an ultrasonic device for one minute. The samples were then floated between two glass chambers using a centrifugal pump. In the end, the sample was placed under a neon–helium laser beam with a wavelength of 632.8 nm, and the resolution was performed. Using Hoffmann's theory, the particle diameter was calculated using Eq. (1). The device used in this process was made by Fritz Co., Germany [37].

$$D = (1.22F\lambda)/R_{\mathrm{o}} \tag{1}$$

where $D$ is the particle diameter; $\lambda$, wavelength, 623.8 nm; $R_{\mathrm{o}}$, radius of the device ring; and $F$, frequency.

To investigate the geotechnical and geoenvironmental behavior of the samples at pHs of 2, 4, 6, 8.5 (natural marl) and 11, experiments of Atterberg Limits [38], permeability [39] and unrestricted compressive strength [40] were performed.

The permeability coefficient was measured by the falling head method [39]. Soil samples passing through sieve no. 40 with maximum specific gravity and optimum moisture content was pounded in $5 \times 10$ cm molds in 3 layers made of PVC. After samples were saturated (after about 1 month), a permeability test was performed on all samples.

To determine the unconfined compressive strength of marl samples at pHs of 2, 4, 6, 8.5 and 11, a uniaxial test [40] by control strain method with a loading speed of 0.1 mm/s was performed by ARRAY SH-300 uniaxial compressive strength tester. To prepare the samples, the soil passing through the sieve no. 40 with maximum specific gravity and optimum moisture content were pounded in molds with dimensions of $5 \times 9.5$ cm in 3 layers and the samples were stored in plastic containers at a constant humidity to reach equilibrium for 72 h. Finally, all compressive strength tests for each sample were repeated with 4 different samples.

To prepare the sample for the XRD test, 5gr of each powdered dry soil sample was weighed with an accuracy of 0.001, and the samples were exposed to radiation at the wavelength of 1.54 Å (corresponding to kα of element Cu). Samples were tested using X-ray diffractometer (D8-ADVANCE) made by Bruker, Germany [41]. The XRD spectrum was examined with a 2ɵ scan in the range of 2°–60°. All the XRD tests for each sample were repeated with 2 different samples.

The results of the XRD test indicate that the main clay minerals of natural marl soil include kaolinite ($d = 7.04$ Å), palygorskite ($d = 9.87$ Å) and sepiolite ($d = 3.53$ Å) and non-clayey minerals include quartz ($d = 3.33$ Å) and calcite ($d = 3.02$ Å) (Fig. 1).

To obtain the images of scanning electron microscopy (SEM), 1 g of each sample of powdered soil was weighed with an accuracy of 0.001 g. The gold plating was used to make the samples conductive and prepare them for testing. It is worth mentioning that the samples were analyzed by TESCAN vega3.

## 3 Results and Discussion

### 3.1 Effect of Initial pH Changes on the Carbonate Content in the Marl

After the marl samples were stabilized at pHs 2, 4, 6, 8.5 and 11, the carbonate content in each sample was determined as a percentage by titration test.

Figure 2 shows the CaO content in marl samples with different initial pH obtained using XRF analysis and the percentage of carbonate obtained from the titration experiment. The carbonate content in natural marl is 31%. The carbonate content of the soil decreases with the decrease in its initial pH. At the initial pH of 4, the carbonate content has reached about 1.5%. According to [42], carbonate can be stable in acidic environments up to pH 3.5.

In the marl sample with an initial pH of 2, calcium carbonate is completely removed from the soil structure and reduced to zero. The addition of sodium hydroxide (NaOH)

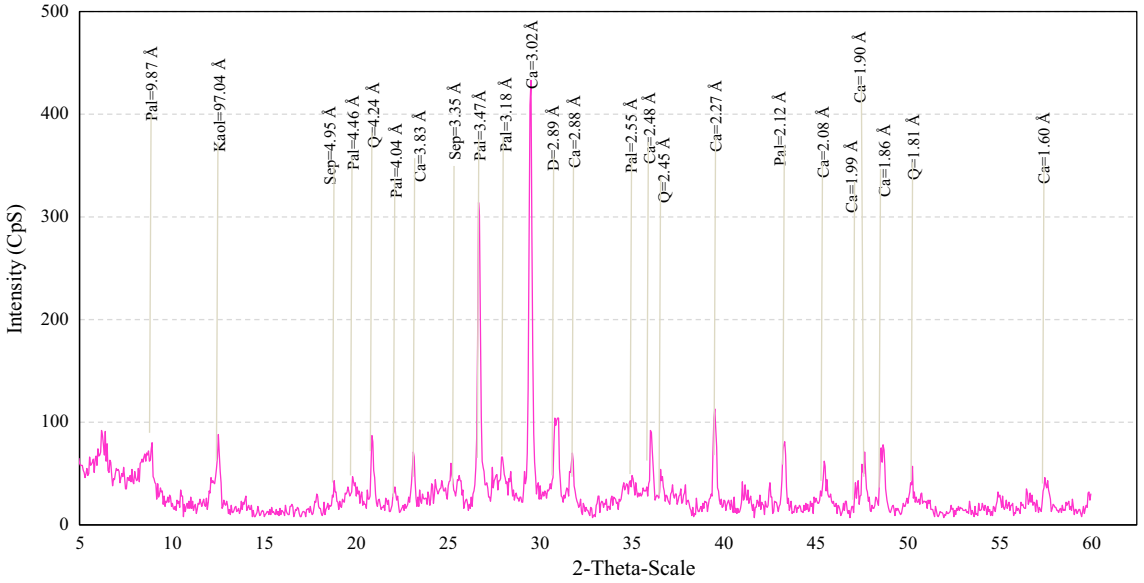


**Fig. 1** X-ray diffraction (XRD) of marl (pH = 8.5). Kaol: Kaolinite; Pal: palygorskite; Sep: sepiolite; Q: quartz; Ca: calcite; D: dolomite

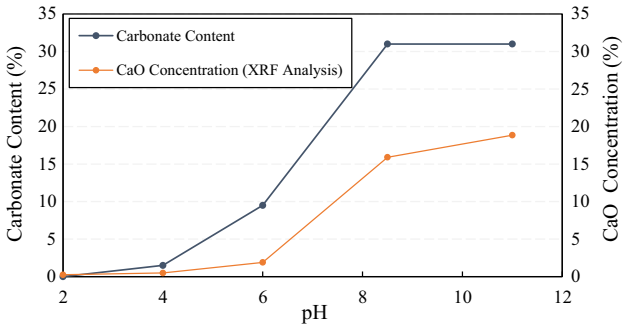


**Fig. 2** Carbonate content changes in marl at different initial pHs

and increase in soil pH did not affect the carbonate content of the soil. Based on Eqs. (2) and (3), with the use of calcium carbonate and magnesium carbonate along with hydrochloric acid (HCl), a bond is formed between chloride ion ($Cl^-$) and the cations of calcium ($Ca^{2+}$) and magnesium ($Mg^{2+}$) and calcium chloride ($CaCl_2$) and magnesium chloride ($MgCl_2$) are obtained. The resulting compounds are water-soluble and are released from the soil structure in the presence of water, and as the sample dries, the resulting carbon dioxide ($CO_2$) is released as vapor and water ($H_2O$).

$$CaCO_3 + 2HCl \rightarrow CaCl_2 + CO_2 + H_2O \quad (2)$$

$$MgCO_3 + 2HCl \rightarrow MgCl_2 + CO_2 + H_2O \quad (3)$$

Table 4 presents the XRF chemical analysis of marl samples with different initial pH. Based on the presented analysis, the amount of calcium oxide and magnesium oxide in natural marl is reported to be 15.91% and 6.02%, respectively.

**Table 4** Chemical properties of marl in southern Iran based on XRF

| Composition (%) | pH | | | | |
|---|---|---|---|---|---|
| | 2 | 4 | 6 | 8.5 (natural marl) | 11 |
| $SiO_2$ | 56.19 | 47.63 | 47.17 | 33.46 | 34.61 |
| $Al_2O_3$ | 11.05 | 12.15 | 12.37 | 9.32 | 9.79 |
| $Fe_2O_3$ | 2.82 | 6.13 | 6.20 | 4.48 | 4.08 |
| $K_2O$ | 2.36 | 5.60 | 1.97 | 1.57 | 1.50 |
| MgO | 1.92 | 1.91 | 6.49 | 6.02 | 6.32 |
| $Na_2O$ | 1.17 | 1.5 | – | 3.21 | – |
| $TiO_2$ | 0.76 | 0.55 | 0.62 | 0.44 | – |
| CaO | 0.25 | 0.49 | 1.90 | 15.91 | 18.85 |
| $SO_3$ | – | – | – | 0.67 | – |
| $P_2O_5$ | – | – | – | 0.14 | – |
| Cl | – | – | – | 1.15 | – |
| LOI | 23.48 | 24.04 | 23.28 | 23.63 | 24.85 |

In the sample with an initial pH of 2, the amount of these elements is decreased by 0.25 and 1.92%, respectively. The results of the XRF analysis confirm the test results for carbonate content determination. The results of XRF and titration experiments show that the carbonate in the marl is removed from the soil structure by HCl, while the alkaline conditions and the amount of NaOH do not affect the carbonate content in the marl.

Regarding the difference in the percentage of carbonate in the XRF analysis and the titration test, it should be noted that the results of the titration test include a collection of carbonates in the marl. XRF analysis, on the other hand, reports

only the calcium carbonate content in the marl. Based on XRF analysis, the amount of silicate ($SiO_2$) in acidic samples has increased, so that in the sample with an initial pH 2, it has reached 56.19%. The alumina in the sample with an initial pH 2 also decreased due to the complete removal of carbonate from the soil structure and the dissolution of alumina at pH ≤ 4. In the sample with an initial pH of 11, the amount of alumina decreased by 1.03 units. The dissolution diagram of silica and alumina proposed by [43] can be a good justification for the results obtained using XRF analysis.

### 3.2 Evaluation of X-ray Diffraction Changes in Marl at Different Initial pHs

Figure 3a presents the results of the XRD test. In natural marls, the intensity of the main peak of calcium carbonate ($d = 3.02$ Å) is 433 CpS. In the sample with an initial pH of 6, the intensity of the peak was reduced to 44 CpS. In samples with an initial pH of 4 and 2, calcium carbonate peaks are completely removed. Examination of the sample with an initial pH 11 showed that the peak related to calcium carbonate ($d = 3.02$ Å) had slightly increased [44, 45].

The peak intensity of dolomite ($d = 2.89$ Å) is equal to 104 CpS. In the sample with an initial pH of 6, the intensity did not change significantly. In samples with an initial pH of 4 and 2, this peak intensity is significantly reduced. The removal of calcium carbonate and dolomite peaks in samples with pH 4 and 2 confirms the carbon dioxide test results and Table 4.

In natural marls, the peak of palygorskite ($d = 9.87$ Å) is observed with an intensity of 80 CpS. The intensity of this mineral in acidic samples 6, 4 and 2 increased by 1.45, 1.5 and 1.8, respectively, so that its intensity in the sample with an initial pH of 2 reached 144 CpS. Due to the removal of the calcium carbonate peaks in the marl, which were regarded as caps on the minerals, the intensity of the palygorskite peak in acidic samples is increased. In the alkaline sample (pH = 11), no significant change in the peak intensity of this mineral is observed. In general, it can be said that with changes in pH (from 2 to 11), the crystal structure of palygorskite minerals will be stable.

The intensity of the main peak of sepiolite ($d = 3.53$ Å) is about 60 CpS in natural marl (pH = 8.5). The peak intensity in samples with initial pH 6 and 4 increased to 94 CpS and 102 CpS, respectively. However, in the sample with an initial pH of 2, the peak intensity decreased to 57 CpS. In the alkaline sample with an initial pH of 11, the peak intensity did not change significantly and remained constant. The continuous dissolution rate of the sepiolite depends on the stability of the Si and Mg concentrations. Based on the XRF results in Table 4, at pH 2 and 4, the MgO content decreased, which is in good agreement with the decrease in the peak intensity of sepiolite. Based on studies and experiments by [46], dissolution of sepiolite is incompatible with both acid and alkali environments and does not follow a specific trend [44, 46, 47].

The intensity of the main peak of kaolinite ($d = 7.04$ Å) is 88 CpS. In samples with initial pH 6 and 4, the kaolinite peak intensities increased by 140 CpS and 150 CpS, respectively. This increase was due to the removal of carbonate from the soil structure. However, the kaolinite peak in the sample with an initial pH 2 was removed due to the dissolution of the clay mineral structure. As the pH increases from 2 to 8, the solubility of kaolinite decreases. In fact, in acidic environments, the dissolution rate of kaolinite is higher, and at 8 ≤ pH ≤ 9, the dissolution of kaolinite is pH-independent. The solubility of kaolinite increases slightly at 9 ≤ pH ≤ 11. The dissolution rate of kaolinite is relatively directly related to the adsorption of $H^+$ and $OH^-$ ions on the oxide surface [44, 48–50]. Since the dissolution rate of kaolinite is dependent on Al and in the pH range of 8.5–11, according to XRF results, the $Al_2O_3$ content slightly decreased. Accordingly, the rate of change of the main peak of kaolinite is negligible [48].

By removing the calcium carbonate from the sample with an initial pH 4 and 2, an increase in the peak intensity of quartz is observed in ($d = 3.33$ Å) and ($d = 4.24$ Å), in such a way that the sample with the initial pH 4, the peak intensity of quartz ($d = 3.33$ Å) reached 583 CpS from 314 CpS, and in the sample with initial pH 2, it reached 907 CpS. The dissolution rate of quartz is measured by the release rate of silica into the solution and is independent of pH changes. The effect of pH on quartz dissolution will be based on equilibrium constants related to silica ionization. Ionization reaction at pH < 7 will be negligible, and in an acidic environment, the pH will not affect the solubility of silica [51]. One of the main reasons for the increase in the intensity of quartz peaks in samples with acidic pH is the removal of carbonate from the soil structure. Figure 3b shows the changes in the peak intensity of kaolinite, sepiolite, calcite and quartz at different pHs.

### 3.3 Morphological Study of Marl at Different Initial pHs and Electron Microscopy (SEM)

To investigate the morphological changes of marl in acidic and alkaline environments, SEM images were taken from all samples and the microscopic texture of the samples was analyzed. Figure 4d shows images of natural marl. According to the images, the scattered structure of marl and the bond of clay particles in the vicinity of water, and the presence of white masses of calcium carbonate can be seen due to the effect of the coating on these particles. Palygorskite, sepiolite and kaolinite fibrous minerals with layered structures can be seen in SEM images. Based on these images, quartz crystalline minerals can also be seen in the natural marl samples.

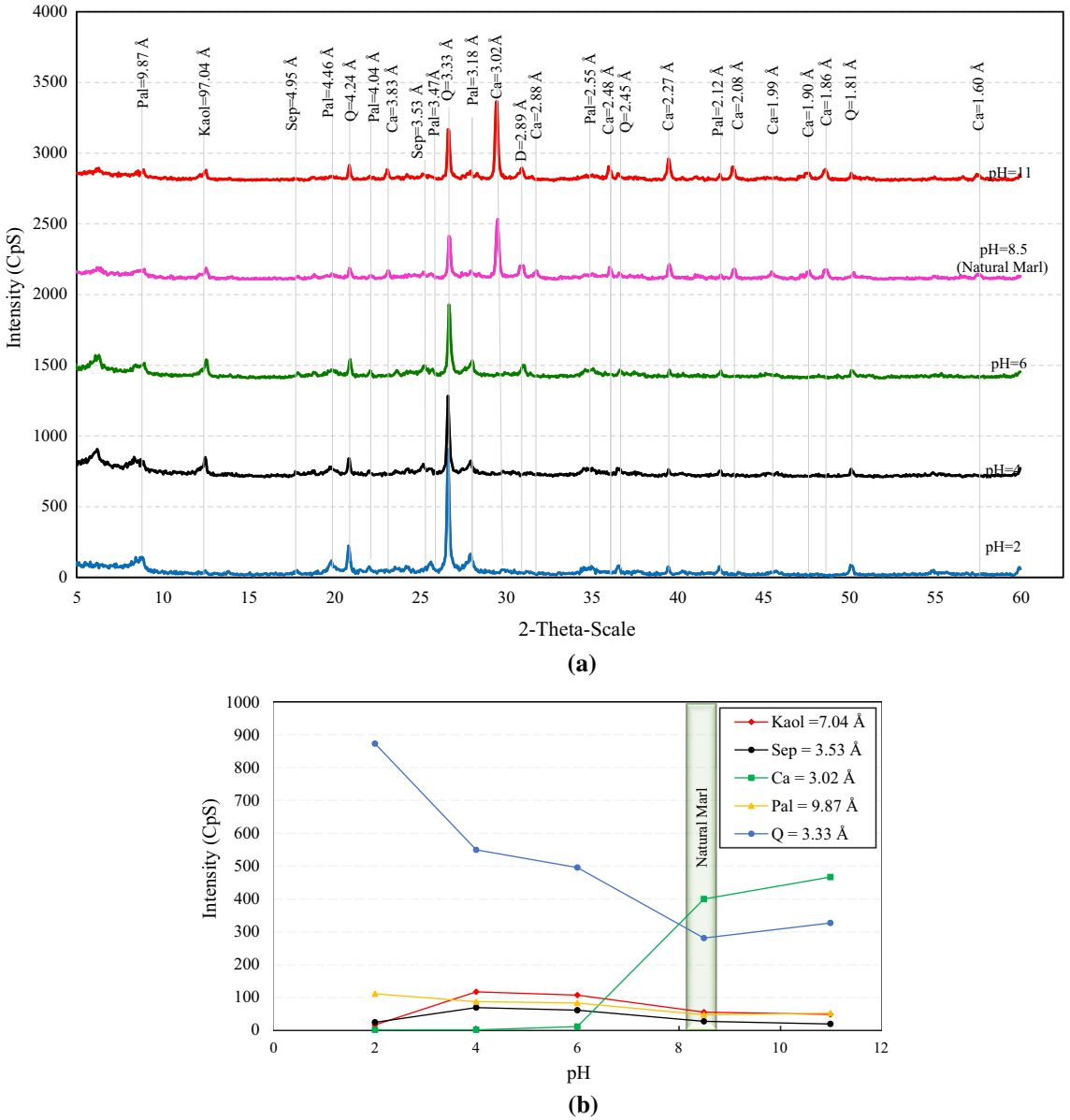


**Fig. 3** **a** X-ray diffraction (XRD) of samples with initial pH 2, 4, 6, 8.5 and 11. **b** Peak intensity changes of samples with initial pH 2, 4, 6, 8.5 and 11. Kaol: Kaolinite, Pal: palygorskite, Sep sepiolite, Q: quartz, Ca: calcite, D: dolomite

As the pH of natural marl decreases, the calcite's mineral content gradually decreases, and in the sample with initial pH 2 and 4 (Fig. 4a, b), this mineral is completely removed.

In an acidic environment, the palygorskite mineral is observed as a cluster of fibrous minerals, and as the pH in the acidic environment increases, the cluster fibers of the palygorskite also diverge and separate. The length of the palygorskite is usually between 1 and 2 μm (μm). As the pH increases, the dispersion of this fibrous mineral increases, and the diameter of the cluster diameter of these minerals decreases [52].

The sepiolite is structurally and chemically similar to the palygorskite, and its fibers run parallel to each other, except that the cell size of the single sepiolite is slightly larger than that of the palygorskite [53–55]. Based on XRD analysis (Fig. 3), the intensity of sepiolite in strongly acidic and alkaline conditions was reduced—which can also be seen in SEM images.

Based on SEM images (Fig. 4b, c), the kaolinite can be observed in samples with initial pH 4 and 6, while in the sample the initial, pH 2 was removed from the soil structure and completely disintegrated, which is consistent with the XRD analysis (Fig. 3). Under alkaline conditions, kaolinite is also observed in soil structure. By reducing the calcium carbonate in the sample with an initial pH of 6, an increase in the quartz is observed in this sample. Also, in the sample with initial

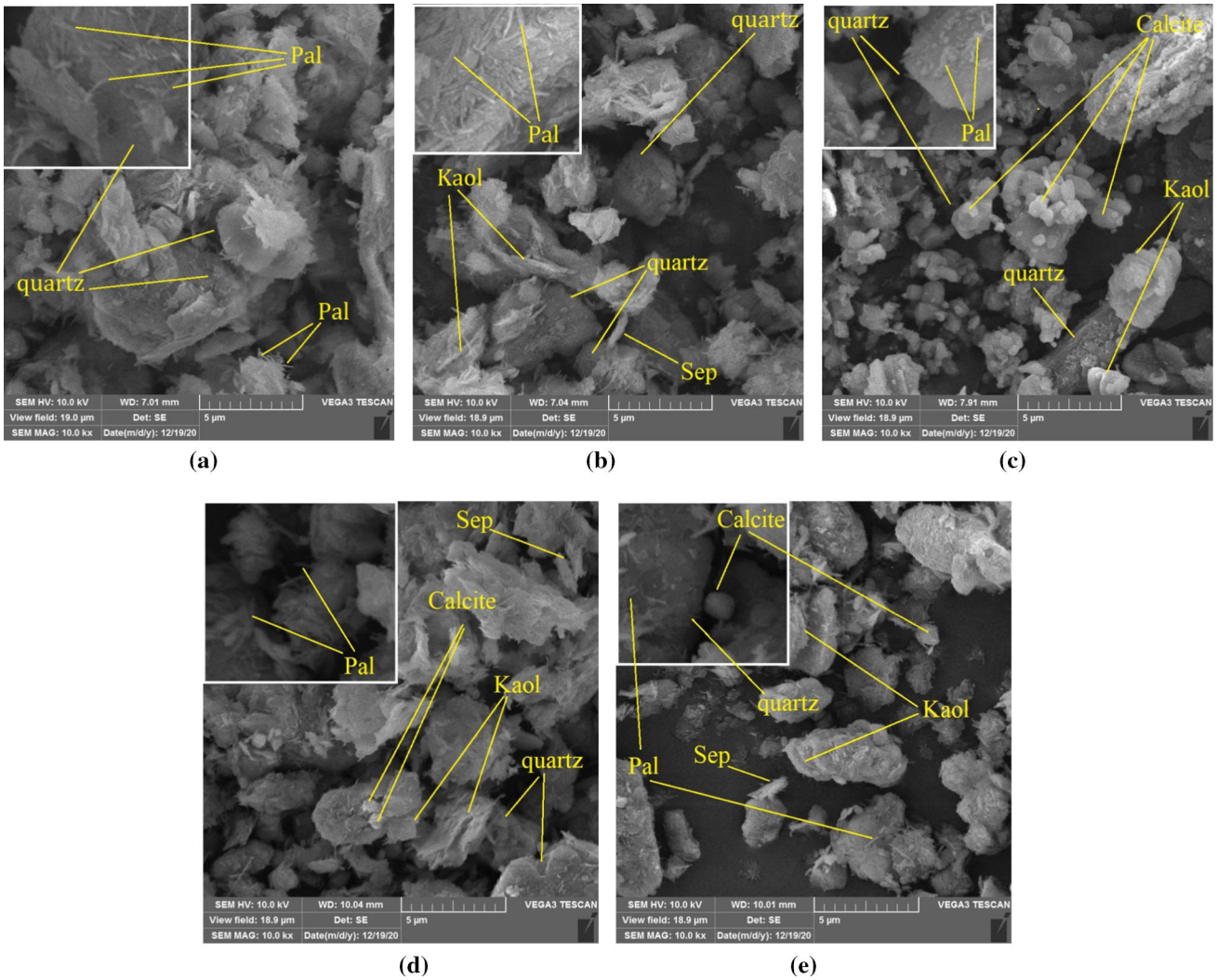


**Fig. 4** SEM image of specimens: **a** pH = 2, **b** pH = 4, **c** pH = 6, **d** natural marl, **e** pH = 11. Kaol: Kaolinite;,Pal: palygorskite, Sep sepiolite, Q: quartz, Ca: calcite, D: dolomite

pH 2 and 4, due to the complete removal of carbonate from the soil structure, in these two samples, the amount of quartz mineral has increased sharply, and in the sample, with initial pH 11, the amount of this mineral has not changed much. Generally, in an acidic environment, the soil structure will be an edge-to-face (E–F) bond. An increased concentration of hydrogen ions creates a positive charge at the edge of the clay platelets, which leads to their adsorption onto the surface containing the negative charge of the other platelets. In this case, the clay particles get closer to each other, and with the increase in the sedimentation rate of the particles, the soil structure becomes aggregated, while the increase in pH and alkaline conditions in the soil causes the particles to disperse (Fig. 4e) [56, 57].

At an initial pH of 11 (Fig. 4e), as the pH of the soil in the alkaline environment increases, the soil structure becomes dispersed relative to the natural marl sample due to an increase in the hydroxide ions content as well as the increase in the negative charge of the clay mineral.

### 3.4 Effect of Different Initial pHs on Soil Particle Size

To determine the particle size distribution of the samples, the results of the laser diffraction particle size analysis (PSA) test are presented in Table 5. According to the presented results, the rate of changes in $D_{20}$ and $D_{50}$ is very small, while that of $D_{90}$ in the sample with initial pH 2 decreased by about 23%, and in the sample with initial pH 11, it decreased by about 15%. According to the analysis, more than 90% of natural marl particles (pH = 8.5) are smaller than 5.36 μm and 88% smaller than 5 μm and the same size as clay particles. At an initial pH of 4, more than 90% of particles have an equivalent diameter smaller than 4.93 μm, and particles the same size as the clay have increased to about 90%. At an initial pH of 2,

**Table 5** Determination of particle diameter range of the studied samples using PSA

| Diameter of particle (μm) | | | | | | |
|---|---|---|---|---|---|---|
| pH | $D_{10}$ | $D_{20}$ | $D_{50}$ | $D_{70}$ | $D_{90}$ | Clay fraction (%) < 5 μm |
| 2 | *** | 1.002 | 2.070 | 2.896 | 4.147 | 96.4 |
| 4 | 0.858 | 1.004 | 2.122 | 3.235 | 4.935 | 90.6 |
| 6 | 0.860 | 1.008 | 2.101 | 3.228 | 5.095 | 89.5 |
| 8.5 (natural marl) | *** | 0.997 | 2.113 | 3.313 | 5.368 | 87.9 |
| 11 | *** | 0.978 | 1.934 | 2.959 | 4.568 | 93.3 |

due to the possibility of aluminum dissolution and disintegration of the structure of clay minerals, more than 90% of soil particles have an equivalent diameter of less than 4.14 μm. It is noteworthy that this 22.5% reduction in particle size compared to natural marl can significantly increase the specific surface area (SSA) as well as the soil plastic parameters. It is worth noting that particles of the same size as clay have increased by about 10% compared to natural marl at initial pH 2.

In acidic environments (pH < 5.5) according to Fig. 4b–d, the soil structure will be in the form of an edge-to-face (E–F) bond. In an acidic environment, due to the absorption of $H^+$ ions, the edge of the particles is positively charged. Particle aggregation can also depend on the thickness of the double layer that forms on the surface of the particles [56, 58]. Significant decrease in the carbonate content and increase in the contact surface of clay particles in the water–soil system are important factors in increasing the content of particles of the same diameter as clay [16].

In an alkaline environment (pH = 11), a decrease in particle size compared to natural marl is observed so that particles of the same size as clay increased by about 5%. In marl with an initial pH of 11, because the edges of clay platelets are negatively charged, the charge of the edge of these particles will be negative due to the adsorption of $OH^-$ ions. Also, due to the dissolution of Al–OH, the soil structure changes from scattered to aggregate (with F–F bonding) [57, 59].

## 3.5 Effect of Initial soil pH Changes on Atterberg Limits and Soil Classification

Atterberg Limits affect the classification of fine-grained soils and the engineering and physical properties of the soil [20]. Based on the results presented in Fig. 5, the liquid limit (LL) and plastic limit (PL) of natural marl are 46 and 25 units, respectively. With the decrease in the initial marl pH to 4, the liquid limit increased to 65 and the plastic limit to 32. In fact, by lowering the pH due to the removal of the carbonate coating (based on the titration results, XRF, XRD and SEM), the contact of clay minerals with the pore water also increases. Based on the results of XRD (Fig. 3) and SEM (Fig. 4), palygorskite is stable in acidic environments. Due

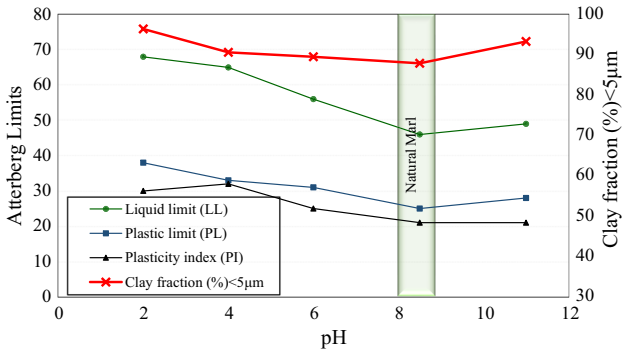


**Fig. 5** Changes of Atterberg Limits in marl at various initial pHs

to the high retention capacity of the pore water of this clayey mineral, the increase in the liquid limit and plastic limit can be justified [52, 60], It is worth noting that these results are consistent with the results of [30, 31]). According to PSA analysis, by decreasing the initial pH of marl, soil particles become smaller, which can increase the liquid limit. At the initial pH of 2, the increase in the liquid limit and plastic limit is observed with a lower slope. Stability of palygorskite, carbonate removal and increase in particle size of clay are the reasons for the increase in the liquid limit and plastic limit.

The acid dissolves the cemented agents between the marl particles. Similarly, [61] showed in their study that the acidic solution could cause the degradation of carbonate (cemented agents between particles) in the soil and its dissolution in the soil structure. Therefore, the effect of increased liquid limit in acidic conditions can be attributed to the mineral compounds in the soil structure and especially the removal of calcium carbonate [20].

In the sample with an initial pH of 11, an increasing trend is observed in the liquid limit and plastic limit of marl, i.e., the liquid limit increased to 49 and the plastic limit to 21. At an initial pH of 11, due to the adsorption of $OH^-$ ions, the edges of the clay platelets will be negatively charged and the soil structure will change from scattered to aggregated (face-to-face-bonded) (F–F) (Fig. 4e) [20, 26]. This is why the liquid limit is increased under alkaline conditions and in the sample with the initial pH of 11.

An increase in the liquid limit and plastic limit increases the plastic index (PI). Therefore, under acidic and alkaline

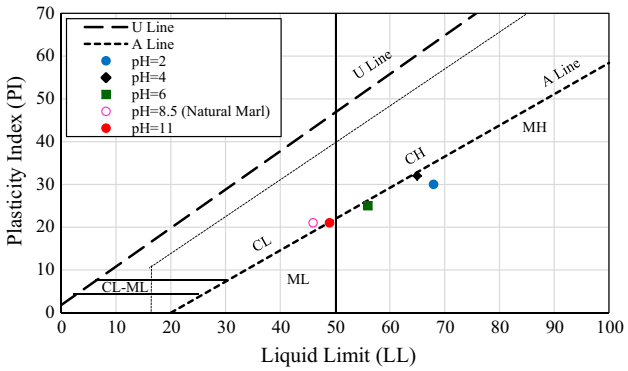


**Fig. 6** Changes in marl classification at different initial pHs according to the plastic diagram

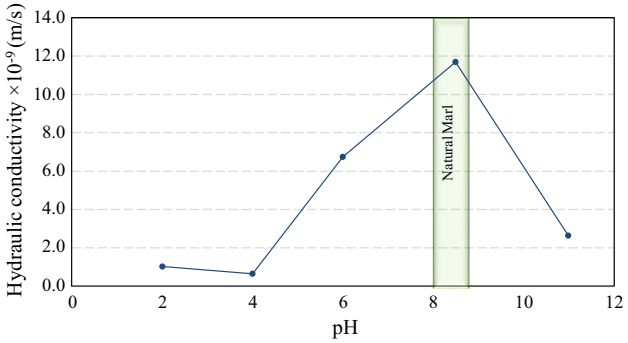


**Fig. 7** Changes in marl permeability coefficient at different initial pHs

conditions, the plastic index of the soil increases (Fig. 5). According to Fig. 5, the maximum plastic index is 32, which is related to the sample with initial pH 4, which has increased by 11 units compared to the natural marl sample.

According to the Unified Soil Classification System (USCS), marls are classified as clay of low plasticity (CL). By changing the initial pH of marl as well as particle size (Table 5) and Atterberg Limits (Fig. 5), soil classification changes and also changes the engineering behavior of marl. By decreasing the initial pH of marl to 6 and 4 through the increase in the liquid limit and plastic limit, according to the plastic diagram in Fig. 6, both samples are close to the A-Line, and the liquid limit of both samples is more than 50 units. Accordingly, soil classification with initial pH 4 and 6 has changed from the clay of low plasticity to the clay of high plasticity/silt of high plasticity (CH/MH). With decreasing pH = 2 and the disintegration of the soil structure due to the dissolution of alumina and, on the other hand, due to the increase in the percentage of particles of the same size as clay, the soil classification switches to silt with high plasticity (MH).

In the alkaline environment (pH = 11), with the increase in the liquid limit and plastic limit, the classification of the soil changes to clay with low plasticity/silt with low plasticity (CL/ML) (Fig. 6). In fact, according to the SEM results, the soil structure has become scattered, due to which the water absorption of clay increases. As a result, the liquid limit and soil classification have also changed [44, 62, 63].

In general, it can be said that the increase or decrease in the initial pH has led to an increase in the liquid limit and plastic limit of marl and a change in soil classification. This change in classification can have a profound effect on the engineering and geoenvironmental behavior of soils.

## 3.6 Effect of Initial Soil pH Changes on Permeability Coefficient

Based on the results of the permeability test, the permeability coefficient of natural marl is $11.7 \times 10^{-9}$ m/s. With decreasing the initial pH = 6, the permeability coefficient decreased to $6.7 \times 10^{-9}$ m/s and this trend continued until the initial pH 4 and the permeability coefficient decreased to $0.61 \times 10^{-9}$ m/s. Based on the results of XRD (Fig. 3) and titration (Fig. 2), with the decrease in pH with increasing particles of the same size as clay as well as the liquid limit and the formation of the complex structure (Fig. 4), the decrease in the permeability could be predicted [64, 65]. In fact, by reducing the particle size, the canals connecting the cavities became very small, and high capillary pressure in the walls of these canals prevented the passage of fluids [66]. In the marl sample with an initial pH 2, the permeability coefficient lowered compared to natural soil (pH = 8.5) and reached $0.99 \times 10^{-9}$ m/s. It is worth noting that the permeability coefficient has increased slightly compared to the initial pH 4, which may be due to the disintegration of the kaolinite structure.

In the marl sample with an initial pH of 11, the permeability coefficient decreased compared to natural soil and reached $2.6 \times 10^{-9}$ m/s. In fact, at pH = 11 (alkaline conditions) the edge of the clay platelet is negatively charged, and therefore, the soil structure is dispersed (Fig. 4e). Under these conditions, an important part of the water in the soil is absorbed by the clay particles, and therefore, their movement or displacement will become difficult. As a result, the permeability is reduced. On the other hand, the stability of palygorskite, sepiolite and kaolinite was another reason for the decrease in permeability coefficient [67, 68] (Fig. 7).

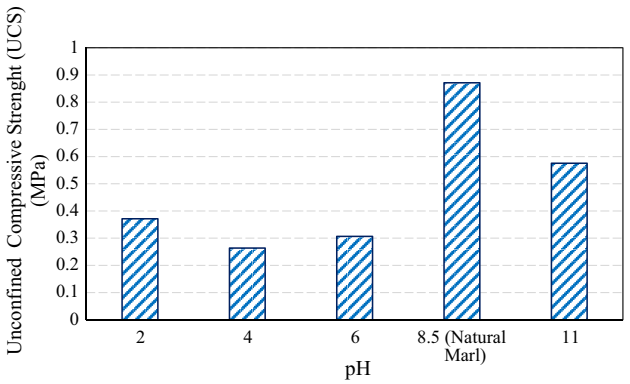


**Fig. 8** Changes in unconfined compressive strength of marls at initial pHs

### 3.7 Changes in Unconfined Compressive Strength of Marl at Different Initial pHs

An unconfined compressive strength test was performed on the samples to investigate the effect of pH, carbonate content and type of clay mineralization on soil resistance behavior. Based on the results, unconfined compressive strength has decreased with increasing and decreasing pH.

According to the results in Fig. 8, the unconfined compressive strength of the natural marl sample is equal to 0.87 MPa. Compressive strength at pHs 6 and 4 decreased by about 65% and 70% to 0.31 MPa and 0.26 MPa, respectively. The reduced carbonate content as a cementing agent between particles and the increased role and intensity of clay minerals in soil behavior are the main reasons for the reduced compressive strength. Based on the results of XRD analysis (Fig. 3) and SEM images (Fig. 4), by lowering the pH and under acidic conditions, the carbonate in the soil dissolves. In addition, the concentration of $H^+$ ions is increased in the pore water of the soil, and due to leaching of soil samples, $Ca^{2+}$ ions are washed out of the soil structure. Therefore, marl shows less resistance in an acidic environment [69].

In the sample with the initial pH 2, the strength of marl increased 1.4 times compared to the sample with initial pH 4 and reached 0.37 MPa. According to the XRF results (Table 4), with increasing acid concentration and decreasing pH, $SiO_2$ increases and $Fe_2O_3$ and $Al_2O_3$ decrease in the soil, which indicates a decrease in the soil's clayey part and carbonate removal. This is the reason for increasing soil strength at this pH compared to a sample with an initial pH of 4 [70].

According to [71], it is also possible for iron oxide to be dissolved by acid, thereby reducing the bonding force between soil particles and the soil strength properties. The compressive strength of the marl sample with initial pH 11 is equal to 0.58 MPa. According to Fig. 3a, because palygorskite is stable under alkaline conditions, the compounds of this mineral have a divergent effect on the soil and a reducing effect on its compressive strength [72].

The presence of ions such as $Al^{3+}$ and $Fe^{3+}$ cause strong bonds between soil particles, and these cations may be leached from the soil during the leaching process. Therefore, the presence or absence of these ions affects the engineering properties of the soil so that in both acidic and alkaline environments, leaching of a high amount of $Ca^{2+}$, $Al^{3+}$ and $Fe^{3+}$ ions from the soil can have a reducing effect on the unconfined compressive strength of the soil [69].

## 4 Conclusion

According to the microstructural analyzes and geotechnical experiments, the results of this study can be summarized as follows:

(a) Changes in microstructural properties of marl are a function of pH, type of clay minerals and carbonate content.
(b) In the $2 \leq pH \leq 11$ range, the crystalline structure of palygorskite is stable.
(c) By lowering the pH and under acidic conditions, by removing the carbonate coating (cementing agent between the particles), the contact of clay minerals with the pore water increases, and considering the stability of palygorskite mineral and the high retention capacity of the pore water in this clayey mineral, the liquid limit and plastic limit are increased.
(d) The presence of ions such as $Al^{3+}$ and $Fe^{3+}$ cause strong bonds between soil particles, and due to the leaching of these cations which leave the soil structure in the leaching process, the unconfined compressive strength of the soil is reduced by about 70%.
(e) The unconfined compressive strength of the natural marl sample is 0.87 MPa. Compressive strength at initial pH 4 decreased to about 70% and reached 0.26 MPa. The reduced carbonate content as a cementing agent between particles and the increased role and intensity of clay minerals in soil behavior are the main reasons for the reduced compressive strength.
(f) According to the permeability test, the permeability coefficient of natural marl is $11.7 \times 10^{-9}$ m/s, and by decreasing the pH to 4, the permeability coefficient is reduced 10 times to $0.99 \times 10^{-9}$ m/s. In fact, by reducing the particle size of the canals connecting the cavities, they become very small, and high capillary pressure in the walls of these canals prevents the passage of fluids.
(g) The increased or decreased initial pH has led to an increase in the liquid and plastic limit of marl and a change in soil classification. This classification change has a strong impact on the engineering and geoenvironmental behavior of soils.

**Acknowledgements** The authors would like to thank the University of Hormozgan, which supported the expenses for all the tests conducted in this study.

**Funding** This research was funded by the University of Hormozgan of Iran (2018Y453214).

**Availability of data and materials** The datasets generated during and/or analyzed during the current study are available from the corresponding author on reasonable request.

## Declarations

**Conflict of interest** The authors declare that they have no conflict of interest.

**Ethical Approval** As the corresponding author on behalf of all the authors, we assure you that this manuscript did not submit to another journal at the same time.

**Consent to Participate** All authors agree to publish the article.

**Consent to Publish** All authors agree to publish the article.

## References

1. Benyahia, S.; Boumezbeur, A.; Lamouri, B.; Fagel, N.: Swelling properties and lime stabilization of N'Gaous expansive marls, NE Algeria. J. Afr. Earth Sci. (2020). https://doi.org/10.1016/j.jafrearsci.2020.103895
2. Singer, A.; Huertos, E.G.; Galan, E.: Developments in Palygorskite-Sepiolite Research: A New Outlook on these Nanomaterials. Elsevier, Amsterdam (2011)
3. Eberhardt, E.; Thuro, K.; Luginbuehl, M.: Slope instability mechanisms in dipping interbedded conglomerates and weathered marls—the 1999 Rufi landslide, Switzerland. Eng. Geol. **77**(1–2), 35–56 (2005). https://doi.org/10.1016/j.enggeo.2004.08.004
4. Wüst, R.A.; McLane, J.: Rock deterioration in the royal tomb of Seti I, Valley of the Kings, Luxor, Egypt. Eng. Geol. **58**(2), 163–190 (2000). https://doi.org/10.1016/S0013-7952(00)00057-0
5. Amiri, M.; Kalantari, B.; Dehghanih, M.; Porhonar, F.; Papi, M.; Salehian, R., et al.: Microstructural investigation of changes in engineering properties of heated lime-stabilized marl soil. Proc. Inst. Civ. Eng. Ground Improv. (2021). https://doi.org/10.1680/jgrim.20.00039
6. Sadeghi, S.H.; Hazbavi, Z.; Kiani-Harchegani, M.; Younesi, H.; Sadeghi, P.; Angulo-Jaramillo, R., et al.: The hydrologic behavior of Loess and Marl soils in response to biochar and polyacrylamide mulching under laboratorial rainfall simulation conditions. J. Hydrol. **592**, 125620 (2021). https://doi.org/10.1016/j.jhydrol.2020.125620
7. Bensaifi, E.; Bouteldja, F.; Nouaouria, M.; Breul, P.: Influence of crushed granulated blast furnace slag and calcined eggshell waste on mechanical properties of a compacted marl. Transp. Geotech. **20**, 100244 (2019). https://doi.org/10.1016/j.trgeo.2019.100244
8. Elert, K.; Azañón, J.M.; Nieto, F.: Smectite formation upon lime stabilization of expansive marls. Appl. Clay Sci. **158**, 29–36 (2018). https://doi.org/10.1016/j.clay.2018.03.014
9. Ouhadi, V.; Yong, R.: Impact of clay microstructure and mass absorption coefficient on the quantitative mineral identification by XRD analysis. Appl. Clay Sci. **23**(1–4), 141–148 (2003). https://doi.org/10.1016/S0169-1317(03)00096-6
10. Lamas, F.; Irigaray, C.; Oteo, C.; Chacon, J.: Selection of the most appropriate method to determine the carbonate content for engineering purposes with particular regard to marls. Eng. Geol. **81**(1), 32–41 (2005). https://doi.org/10.1016/j.enggeo.2005.07.005
11. Yu, Y.; Ji, Y.; Lu, J.; Yin, X.; Zhou, Q.: Degradation of sulfamethoxazole by $Co_3O_4$-palygorskite composites activated peroxymonosulfate oxidation. Chem. Eng. J. (2021). https://doi.org/10.1016/j.cej.2020.126759
12. Li, X.; Ni, C.; Lu, X.; Zuo, S.; Liu, W.; Yao, C.: In situ fabrication of Ce 1–x La x O 2− δ/palygorskite nanocomposites for efficient catalytic oxidation of CO: effect of La doping. Catal. Sci. Technol. **6**(2), 545–554 (2016)
13. Zhang, L.; Lv, F.; Zhang, W.; Li, R.; Zhong, H.; Zhao, Y., et al.: Photo degradation of methyl orange by attapulgite–$SnO_2$–$TiO_2$ nanocomposites. J. Hazard. Mater. **171**(1–3), 294–300 (2009). https://doi.org/10.1016/j.jhazmat.2009.05.140
14. Potgieter, J.; Potgieter-Vermaak, S.; Kalibantonga, P.: Heavy metals removal from solution by palygorskite clay. Miner. Eng. **19**(5), 463–470 (2006). https://doi.org/10.1016/j.mineng.2005.07.004
15. Mazzullo, S.: Calcite pseudospar replacive of marine acicular aragonite, and implications for aragonite cement diagenesis. J. Sediment. Res. **50**(2), 409–422 (1980). https://doi.org/10.1306/212F7A18-2B24-11D7-8648000102C1865D
16. Yong, R.N.: Geoenvironmental Engineering: Contaminated Soils, Pollutant Fate, and Mitigation. CRC Press, Boca Raton (2000)
17. Benhaddya, M.L.; Hadjel, M.: Spatial distribution and contamination assessment of heavy metals in surface soils of Hassi Messaoud, Algeria. Environ. Earth Sci. **71**(3), 1473–1486 (2014). https://doi.org/10.1007/s12665-013-2552-3
18. Chen, X.; Lu, X.; Li, L.Y.; Yang, G.: Spatial distribution and contamination assessment of heavy metals in urban topsoil from inside the Xi'an second ringroad, NW China. Environ. Earth Sci. **68**(7), 1979–1988 (2013). https://doi.org/10.1007/s12665-012-1885-7
19. Amiri, M.; Dehghani, M.; Javadzadeh, T.; Taheri, S.: Effects of lead contaminants on engineering properties of Iranian marl soil from the microstructural perspective. Miner. Eng. **176**, 107310 (2022). https://doi.org/10.1016/j.mineng.2021.107310
20. Koupai, J.A.; Fatahizadeh, M.; Mosaddeghi, M.R.: Effect of pore water pH on mechanical properties of clay soil. Bull. Eng. Geol. Environ. **79**(3), 1461–1469 (2020). https://doi.org/10.1007/s10064-019-01611-1
21. Wang, X.; Huang, L.; Yan, C.; Lian, B.: HKCV rheological constitutive model of mudstone under dry and saturated conditions. Adv. Civ. Eng. (2018). https://doi.org/10.1155/2018/2621658
22. Siddiqua, S.; Bigdeli, A.; Cherian, C.: Effect of pore fluid pH on the collapse behaviour and microstructural evolution of a loess. Environ. Geotech. **40**, 1–11 (2020)
23. Tiwari, B.; Ajmera, B.: Effects of saline fluid on compressibility of clay minerals. Environ. Geotech. **1**(2), 108–120 (2014)
24. Deng, Y.; Yue, X.; Cui, Y.-J.; Shao, G.; Liu, S.; Zhang, D.: Effect of pore water chemistry on the hydro-mechanical behaviour of Lianyungang soft marine clay. Appl. Clay Sci. **95**, 167–175 (2014). https://doi.org/10.1016/j.clay.2014.04.007
25. Nguyen, X.-P.; Cui, Y.-J.; Tang, A.M.; Deng, Y.; Li, X.-L.; Wouters, L.: Effects of pore water chemical composition on the hydro-mechanical behavior of natural stiff clays. Eng. Geol. **166**, 52–64 (2013). https://doi.org/10.1016/j.enggeo.2013.08.009
26. Gratchev, I.B.; Sassa, K.: Cyclic behavior of fine-grained soils at different pH values. J. Geotech. Geoenviron. Eng. **135**(2), 271–279 (2009)
27. Martin, R.T.; Lambe, T.W.: soil composition and its influence on the engineering behaviour of fine-grained soils. Clay Miner. Bull. **3**(17), 137–150 (1957). https://doi.org/10.1180/claymin.1957.003.17.04

28. Spagnoli, G.; Rubinos, D.; Stanjek, H.; Fernández-Steeger, T.; Feinendegen, M.; Azzam, R.: Undrained shear strength of clays as modified by pH variations. Bull. Eng. Geol. Environ. **71**(1), 135–148 (2012). https://doi.org/10.1007/s10064-011-0372-9
29. Jozefaciuk, G.; Sokołowska, Z.; Sokołowski, S.; Alekseev, A.; Alekseeva, T.: Changes of mineralogical and surface properties of water dispersible clay after acid treatment of soils. Clay Miner. **30**(2), 149–155 (1995). https://doi.org/10.1180/claymin.1995.030.2.06
30. Gadouri, H.; Harichane, K.; Ghrici, M.: Assessment of sulphates effect on the classification of soil–lime–natural pozzolana mixtures based on the Unified Soil Classification System (USCS). Int. J. Geotech. Eng. **12**(3), 293–301 (2018). https://doi.org/10.1080/19386362.2016.1275429
31. Gadouri, H.; Harichane, K.; Ghrici, M.: Assessment of sulphates effect on pH and pozzolanic reactions of soil–lime–natural pozzolana mixtures. Int. J. Pavement Eng. **20**(7), 761–774 (2019). https://doi.org/10.1080/10298436.2017.1337119
32. Glatstein, D.; Francisca, F.: Influence of pH and ionic strength on Cd, Cu and Pb removal from water by adsorption in Na-bentonite. Appl. Clay Sci. **118**, 61–67 (2015). https://doi.org/10.1016/j.clay.2015.09.003
33. Palomino, A.; Santamarina, J.: Fabric map for kaolinite: effects of pH and ionic concentration on behavior. Clays Clay Miner. **53**(3), 211–223 (2005). https://doi.org/10.1346/CCMN.2005.0530302
34. Mitchell, J.; Madsen, F.: Chemical effects on clay hydraulic conductivity. In: Geotechnical Practice for Waste Disposal'87, pp. 87–116. ASCE (1987)
35. Hesse, P.R.: A Textbook of Soil Chemical Analysis. John Murray, London (1971)
36. ASTM C1070-01: Standard Test Method for Determining Particle Size Distribution of Alumina or Quartz by Laser Light Scattering (2014)
37. Oudadi, V.; Amiri, M.: Segregation of bentonite components in order to achieve nano montmorillonite. Iran. J. Crystallogr. Mineral. **20**(4), 677–684 (2012)
38. ASTM D4318: Standard Test Methods for Liquid Limit, Plastic Limit, and Plasticity Index of Soils. ASTM International, West Conshohocken (2000)
39. ASTM D5084: Standard Test Methods for Measurement of Hydraulic Conductivity of Saturated Porous Materials Using a Flexible Wall Permeameter. ASTM International, West Conshohocken (2016)
40. ASTM D2166: Standard Test Method for Unconfined Compressive Strength of Cohesive Soil. ASTM International, West Conshohocken (2006)
41. Ichimura, A.; Manning, B.: Bruker D8 Advance Powder XRD Instrument Manual and Standard Operating Procedure (SOP). San Francisco State University, San Francisco (2004)
42. Chen, X.; Achal, V.: Effect of simulated acid rain on the stability of calcium carbonate immobilized by microbial carbonate precipitation. J. Environ. Manag. **264**, 110419 (2020)
43. Keller, W.: The origin of high-alumina clay minerals: a review. Clays Clay Miner. **12**(1), 129–151 (1963)
44. Mitchell, J.K.; Soga, K.: Fundamentals of Soil Behavior, p. 422. Wiley, New York (1993)
45. Althoff, P.: Structural refinements of dolomite and a magnesian calcite and implications for dolomite formation in the marine environment. Am. Mineral. **62**(7–8), 772–783 (1977)
46. Mulders, J.J.; Oelkers, E.H.: An experimental study of sepiolite dissolution rates and mechanisms at 25 °C. Geochim. Cosmochim. Acta **270**, 296–312 (2020). https://doi.org/10.1016/j.gca.2019.11.026
47. Post, J.E.; Bish, D.L.; Heaney, P.J.: Synchrotron powder X-ray diffraction study of the structure and dehydration behavior of sepiolite. Am. Mineral. **92**(1), 91–97 (2007). https://doi.org/10.2138/am.2007.2134
48. Carroll-Webb, S.A.; Walther, J.V.: A surface complex reaction model for the pH-dependence of corundum and kaolinite dissolution rates. Geochim. Cosmochim. Acta **52**(11), 2609–2623 (1988). https://doi.org/10.1016/0016-7037(88)90030-0
49. Downs, R.T.; Bartelehs, K.L.; Gibbs, G.V.: Interactive software for calculating and displaying X-ray or neutron powder diffractometer patterns of crystalline materials. Am. Mineral. **78**, 1104–1107 (1993)
50. Ouhadi, V.; BahadoriNezhad, O.; Amiri, M.: Lead retention of carbonated kaolinite in the adsorption and electrokinetics processes. Modares Civ. Eng. J. (M.C.E.J.) **14**(2), 17–30 (2014)
51. Knauss, K.G.; Wolery, T.J.: The dissolution kinetics of quartz as a function of pH and time at 70 C. Geochim. Cosmochim. Acta **52**(1), 43–53 (1988). https://doi.org/10.1016/0016-7037(88)90055-5
52. Cui, J.; Zhang, Z.; Han, F.: Effects of pH on the gel properties of montmorillonite, palygorskite and montmorillonite-palygorskite composite clay. Appl. Clay Sci. **190**, 105543 (2020). https://doi.org/10.1016/j.clay.2020.105543
53. Guggenheim, S.; Adams, J.; Bain, D.; Bergaya, F.; Brigatti, M.F.; Drits, V., et al.: Summary of recommendations of nomenclature committees relevant to clay mineralogy: report of the Association Internationale pour l'Etude des Argiles (AIPEA) Nomenclature Committee for 2006. Clays Clay Miner. **54**(6), 761–772 (2006)
54. Krekeler, M.P.; Guggenheim, S.: Defects in microstructure in palygorskite–sepiolite minerals: a transmission electron microscopy (TEM) study. Appl. Clay Sci. **39**(1–2), 98–105 (2008). https://doi.org/10.1016/j.clay.2007.05.001
55. Kyzas, G.; Mitropoulos, A.: Advanced Low-Cost Separation Techniques in Interface Science. Academic Press, Cambridge (2019)
56. Tombácz, E.; Csanaky, C.; Illés, E.: Polydisperse fractal aggregate formation in clay mineral and iron oxide suspensions, pH and ionic strength dependence. Colloid Polym. Sci. **279**(5), 484–492 (2001)
57. Essington, M.: Soil and water chemistry: an integrative approach. CRC Press, Boca Raton (2015)
58. Van Olphen, H.: Clay Colloid Chemistry: For Clay Technologists, Geologists, and Soil Scientists. Krieger, Malabar (1991)
59. Ghobadi, M.; Abdilor, Y.; Babazadeh, R.: Stabilization of clay soils using lime and effect of pH variations on shear strength parameters. Bull. Eng. Geol. Environ. **73**(2), 611–619 (2014). https://doi.org/10.1007/s10064-013-0563-7
60. Ouhadi, V.; Yong, R.: The role of clay fractions of marly soils on their post stabilization failure. Eng. Geol. **70**(3–4), 365–375 (2003). https://doi.org/10.1016/S0013-7952(03)00104-2
61. Imai, G.; Komatsu,Y.; Fukue, M.: Consolidation yield stress of Osaka-Bay pleistocene clay with reference to calcium carbonate contents. In: Contaminated Sediments: Evaluation and Remediation Techniques. ASTM International (2006)
62. Shariatmadari, N.; Yazdanpanah, M.M.; Saeidijam, S.: The effect of sodium chloride solution on swelling, compressibility and permeability of bentonite. J. Eng. Geol. **8**(3), 2261–2276 (2014)
63. Gajo, A.; Maines, M.: Mechanical effects of aqueous solutions of inorganic acids and bases on a natural active clay. Géotechnique **57**(8), 687–699 (2007)
64. Ruhl, J.L.; Daniel, D.E.: Geosynthetic clay liners permeated with chemical solutions and leachates. J. Geotech. Geoenviron. Eng. **123**(4), 369–381 (1997). https://doi.org/10.1061/(ASCE)1090-0241(1997)123:4(369)
65. Nakagawa, T.; Ishiguro, M.: Hydraulic conductivity of an allophanic Andisol as affected by solution pH. J. Environ. Qual. **23**(1), 208–210 (1994). https://doi.org/10.2134/jeq1994.00472425002300010032x
66. Decker, R.; Sherard, J.L.: Dispersive Clays, Related Pipings and Erosion in Geotechnical Projects. ASTM International, West Conshohocken (1977)

67. Anon: The Characteristic of Clay. Groundwater and Environmental Engineering (2003)
68. Athy, L.F.: Density, porosity, and compaction of sedimentary rocks. AAPG Bull. **14**(1), 1–24 (1930)
69. Momeni, M.; Bayat, M.; Ajalloeian, R.: Laboratory investigation on the effects of pH-induced changes on geotechnical characteristics of clay soil. Geomech. Geoeng. (2020). https://doi.org/10.1080/17486025.2020.1716084
70. Barrios, M.S.; González, L.F.; Rodriguez, M.V.; Pozas, J.M.: Acid activation of a palygorskite with HCl: development of physico-chemical, textural and surface properties. Appl. Clay Sci. **10**(3), 247–258 (1995). https://doi.org/10.1016/0169-1317(95)00007-Q
71. Sunil, B.; Nayak, S.; Shrihari, S.: Effect of pH on the geotechnical properties of laterite. Eng. Geol. **85**(1–2), 197–203 (2006). https://doi.org/10.1016/j.enggeo.2005.09.039
72. Neaman, A.; Singer, A.: Flocculation of homoionic sodium palygorskite, palygorskite-montmorillonite mixtures and palygorskite containing soil clays. Soil Sci. **164**(12), 914–921 (1999)